EFFECT OF TEMPERATURE AND REACTION TIME ON THE SYNTHESIS OF NANOCRYSTALLINE BRUCITE

Aránzazu Sierra-Fernandez[1, 2], Luz Stella Gomez-Villalba[1], Lidia Muñoz[2], Gregorio Flores[3], Rafael Fort[1] & Maria Eugenia Rabanal[2]

[1]Instituto de Geociencias (CSIC, UCM), Madrid, Spain.
[2]Universidad Carlos III de Madrid and IAAB, Avda. Universidad 30, 28911 Leganes, Madrid, Spain.
[3]Instituto de Física y Matemáticas, Universidad Tecnológica de la Mixteca, Carretera a Acatlima Km. 2.5, Huajuapan de León, Oaxaca 69000, México.

Corresponding autor: A. Sierra-Fernández, arsierra@ucm.es

Abstract: $Mg(OH)_2$ nanoparticles has been successfully synthesized by means of the hydrothermal method. The effect of the reaction time and the synthesis temperature on the nanoparticles obtained has also been studied. The physic-chemical properties of the synthesized brucite samples have been characterized by X-Ray-diffraction (XRD), scanning electron microscopy/energy dispersive X-rays analysis (SEM/EDX), transmission electron microscopy (TEM), high-resolution transmission electron microscopy (HRTEM), thermogravimetry/ differential scanning Calorimetry (TG-DSC) and in situ high-temperature X-ray diffraction (XRD). The influence of the synthesis parameters in the brucite samples has been discussed in detail. Furthermore, it has been shown that the increase of temperature from 180 to 200ºC improves the crystallinity degree of $Mg(OH)_2$ nanostructured particles and also, promotes the formation of plates with bigger uniform size. As well, the increase in the time reaction induces the formation of bigger size brucite plates. So, this hydrothermal method has been shown to be a really promising method for the large scale production.
Key words: magnesium hydroxide; brucite; hydrothermal method; morphology; crystallization

1. INTRODUCTION

Nowadays, the interest in crystalline magnesium hydroxide ($Mg(OH)_2$) is rapidly growing due to the fact that this important inorganic material has multiple applications in industry (Al-Hazmi et al., 2012), medicine (Janning et al. 2010) or in the conservation of cultural heritage (Gomez-Villalba et al.,2011; Chelazzi et al.,2013) thanks to its physical and chemical properties. Therefore, this metal hydrate offers several great advantages, such as a good thermal stability, good fire retardant properties, a low toxicity and a low cost (Kumari et al., 2009). Furthermore, the nanocrystalline magnesium hydroxide has attracted an important interest for its significant antibacterial activity (Dong et al., 2010). As a new flame retardant, magnesium hydroxide is widely used in different products, such as

polymeric materiales, providing them new important properties and applications (Ulutan et al., 2000; Moreira et al., 2013). In addition, the magnesium hydroxide presents favorable CO_2 adsorption properties (Fagerlund et al., 2011). Recently, Chang et al., 2014 have researched the influence of $Mg(OH)_2$ content on the carbonation process of calcium hydroxide, which provide interesting results on the enhancement of the carbonation efficiency. On the other hand, the nanocrystalline brucite is an important precursor of magnesium oxide (MgO) (Zhang et al., 2014), which has attracted a significant interest due to its high surface reactivity and properties. The method used to obtain the nanoparticles is a key factor to enhance the suitability of these nanomaterials. The control of the synthesis conditions is necessary in order to obtain nanoparticles with specific morphologies, nanometric particle sizes, narrow particle size distribution, appropriate dispersability and crystallographic structures. Therefore, the preparation process of magnesium hydroxide nanoparticles has been the main focus of an important number of studies. So far, $Mg(OH)_2$ nanocrystals with different morphologies, such as nanotubes, hexagonal nanoplates, globular agglomerates or needle-like have been synthesized by means of the solvothermal method (Fan et al., 2003), the bubbling method (Li et al., 2010), the microwave-assisted technique (Beall et al, 2012) or even using the hidrating method of MgO (Qian et al., 2007) and the hydrothermal method (Wang et al., 2014). Among all of them, the hydrothermal synthesis is one the most widely employed techniques for the synthesis of nanocrystalline brucite (Wu et al., 2006). An important number of studies have proven that this method is one of the simplest, effectivest and low-cost way to synthesize brucite crystals (Jin et al., 2008). Our previous studies have focused on the production of $Mg(OH)_2$ nanoparticles by hydrothermal method to a synthesis temperature of 180ºC (Sierra-Fernández, et al. 2014). To our knowledge, additional research are

required to evaluate the influence of synthesis parameters on the properties of the particles obtained in order to make possible the large-scale production of these nanomaterials. Thus, in this study the controlled preparation of $Mg(OH)_2$ nanostructures with different properties, at different synthesis temperature and reaction time has been reported.

2. EXPERIMENTAL CONDITIONS

All the reagents used in this study were analytically pures and were used without further purification. The water used was distilled and desionized. In a typical preparation process, 0.24 g of magnesium nitrate hexahydrate ($Mg(NO_3)_2 \cdot 6H_2O$) was dissolved in 10 ml high-purity water. Then, 2 ml of hydrazine hydrate ($N_2H_4 \cdot H_2O$) were added dropwise to the $Mg(NO_3)_2$ solution under constant stirring. The resulting mixture was vigorously stirred at room temperature until a clear and uniform solution was made. Finally, the obtained solution was transferred into a Teflon-lined stainless steel autoclave, which was sealed and hydrothermally treated at a constant reaction temperature in between the range of 180-200ºC for 12 hours.

The purity and the crystalline structures of synthesized $Mg(OH)_2$ particles were evaluated by the X-ray diffractometer (Philips X´pert) using CuKα radiation (λ=1.54 Å) in the range of 2Θ value between 15° and 70. The average crystallite size of the products was determined from broadening of its main indexed peaks using the Scherrer formula. The formula is $D=K\lambda/\beta\cos\theta$, where λ is the wavelength of the X-ray radiation (in Å), K is a constant taken as 0.9, β the full width at half maximum height (FWHM) and θ is the diffraction angle (in rad) used in calculus. The morphological study and chemical composition of the samples were conducted by Scanning Electron Microscopy (SEM), using a Philips XL 30/EDS D×4, with the surface of the samples coated with a thin gold layer to avoid a charging effect. Transmission electron microscope (TEM, JEOL JEM 2100) and high-resolution transmission electron microscope (HRTEM, JEOL JEM 3000F) analyses were conducted to study the microstructure of the magnesium hydroxide nanoparticles employing an accelerating voltage of 200 kV and 300Kv. Selected area electron diffraction (SAED) was used to confirm the crystalline phases. The samples for TEM and HRTEM studies were ultrasonically dispersed in acetone and then deposited on holey carbon copper grids. The distribution and average size of the nanostructures obtained were determined from TEM images using the Digital MicrographTM (DM, Gatan Inc.) software. Thermogravimetric (TG) and differential scanning calorimetric (DSC) analysis of the magnesium hydroxide particles was carried out on a simultaneous thermal analysis instrument (TGA, DSC Perkin-Elmer STA 6000) from 50 to 900 C with heating rate of 5 C/min^{-1} under N_2 atmosphere (flow rate 20 mL/min). In situ high-temperature X-ray diffraction (XRD) patterns were collected at 25 to 300ºC at intervals of 50ºC, and between 300 and 450ºC at intervals of 25ºC, to 500 and 600ºC with a Philips X'Pert PRO MPD powder diffractometer provided with an Anton Paar HTK 1200 furnace chamber. The samples were heated in an air atmosphere at 10ºC min^{-1} and then allowed to stabilise for 5 min at the required temperature before its XRD was recorded.

3. RESULTS AND DISCUSSION

The crystalline nature of the magnesium hydroxide nanoparticles was confirmed by the analysis of XRD pattern as shown in Fig. 1. This figure shows the X-ray diffraction (XRD) patterns of the as-prepared samples A, B and C obtained by using the hydrothermal method at different synthesis temperatures (180ºC and 200ºC) and reaction times (4 and 12 hours). As it can be seen, these XRD patterns exhibited the characteristic diffraction peaks corresponding to the (001), (101), (102) and (110) planes of the $Mg(OH)_2$ structure (JCPDS no. 44–1482, space group P-$3m1$ with unit cell parameters (a)=3.144 Å and (c)=4.777 Å). No XRD peaks arising from impurities or secondary phases were detected, suggesting a complete synthesis reaction. Nevertheless, the relative intensities of $Mg(OH)_2$ (001) peak are stronger than the diffraction peak for the plane (101).
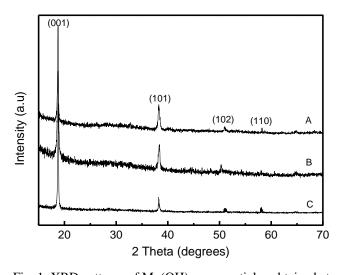

Fig. 1. XRD patterns of $Mg(OH)_2$ nanoparticles obtained at various synthesis conditions. (A) 180ºC, 4 h; (B) 180ºC, 12 h and (C) 200ºC, 12h.

This weakening of the diffraction intensity in the (101) plane could be caused by the preferred growth orientation of the brucite crystals according to the experimental conditions in the synthesis (Wu et al, 2006). In addition, an important increase of the crystallinity degree was detected in the samples

51

obtained at 200ºC. According to Wang et al, (2011) and Chen et al, (2008) the crystallization of the brucite nanoparticles could be improved at higher temperatures. The average grain size could be calculated from the Scherrer´s formula using the most intense peaks, (001) and (101). The results are summarizes in Table 1. As shown, with the increasing of the synthesis temperature and the reaction time, the $Mg(OH)_2$ crystallite size increase from 28 to 48 nm.

Table 1. Variation of crystallite size considering the two most intense diffraction peaks (001) and (101) of the $Mg(OH)_2$ nanoparticles, obtained at precursor quantity of 0,24g of magnesium nitrate hexahydrate $(Mg(NO_3)_2 \cdot 6H_2O)$ and 2 ml of hydrazine hydrate $(N_2H_4 \cdot H_2O)$

Sample	Reaction temperature (ºC)	Reaction Time (h)	Particle size (nm)	Crystallite size (nm)
A	180	4	70 ±30	28±4
B	180	12	200±20	45±4
C	200	12	270±40	48±5

The results of the Scanning Electron Microscopy (SEM) revealed important differences in the particle size and the morphology of the $Mg(OH)_2$ obtained. Fig. 2. shows the SEM micrographs of the $Mg(OH)_2$ nanoparticles. These results showed that the synthesis parameters exercise a strong influence on the morphology and the particle size of the particles obtained. Thus, the image of sample A in Fig. 2a depicts flake shaped particles with the average of the longer side being about ~60 ±20nm and having a thickness of ~8 nm. As it can be seen in Fig.2b, it was possible to observe that with the increase of the time reaction, the size of the sample increased to ~170±30nm. Futhermore, sample B presents well-defined hexagonal nanoflakes, which are consistent with the crystallographic characteristics of $Mg(OH)_2$ (Xue, et al., 2009). Interestingly sample C, in the Fig.2c, shows that the increase of temperature from 180ºC to 200ºC promoted the formation of plates with a bigger and uniform size of ~210±40nm. This increase in the size together with the increase of the temperature has also been observed at temperatures up to 180ºC (Sierra-Fernández et al., 2014). The EDX spectra of the samples show the composition of particles consists of Mg and O elements without any impurities. These results have confirmed a high chemical homogeneity of the magnesium hydroxide samples after analyzing several areas of each sample. The strong X-ray peaks associated with the presence of aluminum (Al) and gold (Au) in the EDX spectra were assigned to the Al bottom and the gold coating deposited in the surface of the samples respectively, which should be ignored.

The morphology and microstructure of the magnesium hydroxide particles have addtional been analyzed by TEM and HRTEM. These data were correlated with the previous results obtained from the XRD and SEM studies. The Fig. 3 (a,b and c) shows the low magnification TEM micrograph of the $Mg(OH)_2$ nanoparticles. Fig. 3a indicates that the sample A, obtained at the synthesis reaction time of 4 hours at 180ºC was composed of particles of ~70 to 100 nm whereas Fig. 3b reveals that sample B are larger hexagonal shape particles (~200±20nm) and more agglomerated.
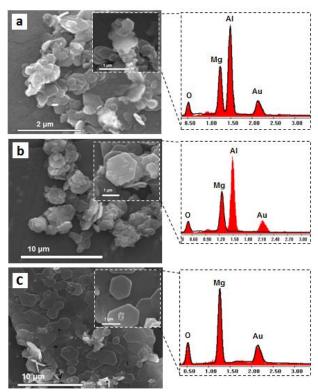

Fig. 2. Scanning electron micrographs of low and the inset at high magnification and EDX analysis of $Mg(OH)_2$ nanoparticles synthesized at (A) 180ºC, 4h; (B) 180ºC, 12h and (C) 200ºC, 12h via hydrothermal method

This tendency to grow the particle sizes with the increase in temperature was also confirmed in sample C. Thus, the increase of temperature from 180ºC to 200ºC was found to lead to the formation of particles with bigger size of ~270±40nm. This progressive increment in the size of particles with the increase in the temperature was also observed by several authors (Xiang et al., 2004; Wu et al., 2006). High resolution transmission electron microscopy (HRTEM) observations were performed in order to study the atomic structure of the magnesium hydroxide samples obtained. The images revealed that the nanoparticles are well cristallized, being somewhat ordered at the atomic scale (Fig.3d and e).

The thermogravimetric analysis (TGA) and the differential scanning calorimetry (DSC) were used to study the thermal decomposition and stability of the magnesium hydroxide nanoparticles. A significant weight loss was observed in the brucite samples when the reaction temperature was higher than 300°C.
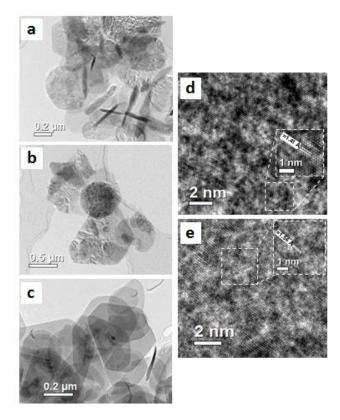
Fig. 3. Low magnification Transmission electron micrographs of Mg(OH)$_2$ nanoparticles obtained at 180ºC for 4 hours (a), 180ºC for 12 hours (b) and 200ºC for 12 hours (c). HRTEM images of the brucite nanoparticles synthesized at 180ºC for 4 hours (d) and 180ºC for 12 hours (e). Inset d and e shows a higher zoom of part of Fig. 3.d and e, respectively.

These weight loss corresponds to the thermal decomposition of dehydroxilation of Mg(OH)$_2$. Fig. 4 shows the TG and DSC curves for the degradation of sample A. As can be seen, the DSC signal shows an endothermic peak, around 368ºC, attributed to the decomposition of brucite at this temperature, which is close to those determined by other authors (Rothon et al., 1996). The weight loss experienced between 343ºC to 388ºC exhibits a 29 wt% weight loss, which is close to the theoretical weight loss of the pure Mg(OH)$_2$(30.8wt%). In addition, in order to study the transition phase process and the effect of the atmosphere on the stability of Mg(OH)$_2$ nanoparticles, the samples were heated in the air and the XRD were recorded. Fig. 5 shows XRD data collected for the sample A over a temperature ramp-up range of 25-600ºC. These results were in concordance with the previous TG-DSC analysis. As it can be seen, all the peaks attributed to the brucite sample, corresponding to the (001), (102) and (110) planes of the brucite phase (Mg(OH)$_2$, JCPDS 44-1482) and, whose intensities decreased throughout the experiment, are in existence before 350ºC. These diffraction peaks attributed to the Mg(OH)$_2$ crystal become undetectable at 375ºC. From this temperate, it can be seen the peaks corresponding to the (200) and (220) planes of the periclase phase (MgO, JCPDS

87-0653), can be seen, confirming the Mg(OH)$_2$ to MgO phase transformation. Therefore, all the magnesium hydroxide nanoparticles obtained showed an important thermal stability with interesting properties for its use as a flame retardant material.
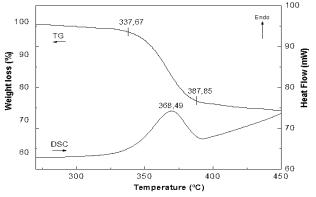

Fig. 4. TG-DSC curves of the thermal decomposition of sample A, heated in nitrogen (N$_2$) flow.
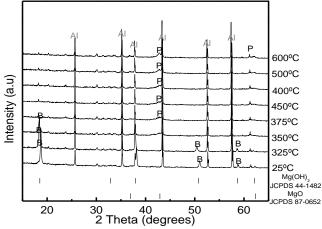

Fig. 5. In situ HXRD patterns of sample A, synthesized at 180ºC for 4 hours. B represents the peaks of brucite (Mg(OH)$_2$), P the peaks of periclase (MgO) and Al the peaks assigned to the diffraction of Alumina (Al$_2$O$_3$) bottom, not considered.

4. CONCLUSIONS

We have successfully synthesized the Mg(OH)$_2$ nanoparticles with different morphologies by hydrothermal method under different temperatures of synthesis and reaction times. All the brucite samples showed the existence of differences in the morphology, particle size, agglomeration level in function of the time reaction and the synthesis temperature. In this way, larger reaction times bring about the growth of well-defined nanoplates of magnesium hydroxide with a bigger and more uniform size with brucite structure. It was also possible to show an important increment of the crystallinity degree and larger particle sizes on the Mg(OH)$_2$ nanoparticles at higher temperatures (200ºC). In addition, the different samples of magnesium hydroxide obtained, showed interesting properties for its use as flame retardant due to its high

thermal stability. The hydrothermal method has proven its effectiveness as a simple and efficient way to obtain $Mg(OH)_2$ nanoparticles of high purity.

ACKNOWLEDGEMENTS

5. REFERENCES

1. Rothon, R.N., Hornsby, P.R., (1996). *Flame retardant effects of magnesium hydroxide*, Polym. Degrad. Stabil., 54, 383-385.

2. Ulutan, S., Gilbert, M., (2000). *Mechanical properties of HDPE/magnesium hydroxide composites*, J. Mater. Sci., 35 (9), 2115-2120.

3. Fan, W., Sun, S., You, L., Cao, G., Song, X., Zhang, W., Yu, H., (2003) *Solvothermal synthesis of Mg (OH)$_2$ nanotubes using $Mg_{10}(OH)_{18}Cl_2 \cdot 5H_2O$ nanowires as precursors*, J. Mater. Chem., 13, 3062-3065.

4. Xiang, L., Jin, Y.C., Jin, Y., (2004). *Hydrothermal formation of dispersive Mg(OH)$_2$ particles in NaOH solution*, Trans. Nonferrous Met. Soc. China., 14, 116-120.

5. Wu, Q.L., Xiang, L., Jin, Y., (2006). *Influence of CaCl$_2$ on the hydrothermal modification of Mg(OH)$_2$*, Powder Technol., 165, 100-104.

6. Qian, H.-y., Deng, M., Zhang, S.-m., Xu, L., (2007). *Synthesis of superfine Mg(OH)$_2$ particles by magnesite*, Mater. Sci. Eng. A-Struct. Mater. Prop. Microstruct. Process., 445-446,600-603.

7. Chen, D., Zhu, L., Zhang, H., Xu, K., Chen, M., (2008). *Magnesium hydroxide nanoparticles with controlled morphologies via wet coprecipitation*, Mater. Chem. Phys., 109, 224-229.

8. Jin, D., Gu, X., Yu, X., Ding, G., Zhu, H., Yao, K., (2008). *Hydrothermal synthesis and characterization of hexagonal Mg(OH)$_2$ nano-flake as a flame retardant*, Mater. Chem. Phys., 112, 962-965.

9. Xue, D., Yan, X., Wang, L., (2009). *Production of specific Mg(OH)2 granules by modifying crystallization conditions*, Powder Technol., 191, 98-106.

10. Kumari, L., Li, W. Z., Vannoy, C., H., Leblanc, R.M., Wang, D.Z., (2009) *Synthesis, Characterization and optical properties of Mg(OH)$_2$ micro-/nanostructure and its conversion to MgO*, Ceram. Int., 35, 3355-3364.

11. Dong, D., Cairney, J., Sun, Q., Maddan, O.L., He, G., Deng, Y., (2010). *Investigation of Mg(OH)$_2$ nanoparticles as an actibacterial agent*, J. Nanopart. Res., 12, 2101-2109.

12. Janning, C., Willbold, E., Vogt, C., Nellesen, J., Meyer-Lindenberg, A., Windhagen, H., Thorey, F., Witte, F., (2010) *Magnesium Hydroxide Temporarily Enhancing Osteoblast Activity and Decreasing the Osteoclast Number in Perimplant Bone Remodelling*, Acta Biomater., 6, 1861-1868.

13. Li; X., Ma, C., Zhao; J., Li; Z., Xu, S., Liu. Y., (2010). *Preparation of magnesium hydroxide nanoplates using a bubbling setup*, Powder Technol., 198, 292-297.

14. Fagerlund, J., Zevenhoven, R.,(2011). *An experimental study of Mg(OH)$_2$ carbonation*, Int. J. Greenh. Gas Control, 5, 1406-1412.

15. Gomez-Villalba, L.S., López-Arce, P., Fort, R., (2011). *Nucleation of CaCO$_3$ polymorphs from a colloidal alcoholic solution of Ca(OH)$_2$ nanocrystals exposed to low humidity conditions*, Appl. Phys. A-Mater. Sci. Process., 106, 213-217.

16. Wang, P., Li, C., Gong, H., Wang, H., Liu, J.,(2011) *Morphology and growth mechanism of magnesium hydroxide nanoparticles via a simple wet precipitation method*, Ceram. Int., 37, 3365-3370.

17. Beall, G.W., Duraia, E.-S.M., Tantawy, F. E.-, Hazmi, F. A, Al- Ghamdi. A.A., (2012) *Rapid fabrication of nanostructured magnesium hydroxide and hydromagnesite via microwave-assisted technique*, Powder Technol., 234, 26-31.

18. Al- Hazmi, F., Umar, A., Dar, G.N., Al-Ghamdi, A.A., Al-Sayari, S.A., Al-Hajry, A., Kim, S.H., Al-Tuwirqi, R.M., Alnowaiserb, F., El-Tantawy, F.,(2012). *Microwave assisted rapid growth of Mg(OH)$_2$ nanosheet networks for ethanol chemical sensor application*, J. Alloy. Compd., 519, 4-8.

19. Chelazzi, D., Poggi, G., Jaidar, Y., Tocaffondi, N., Giorgi, N., Baglioni, P.,(2013). *Hydroxide nanoparticles for cultural heritage: Consolidation and protection of wall paintings and carbonate materials*, J. Colloid Interface Sci., 392, 42-49.

20. Moreira, Francys K.V., Pedro, Daniel C.A., Glenn, Gregory M., Marconcini, José M., Mattodo, Luiz H.C., (2013). *Brucite nanoplates reinforced starch bionanocomposites,* Carbohydr. Polym.,92(2), 1743-1751.

21. Chang, J., Li, Y., Cao, M., Fang, Y. (2014). *Influence of magnesium hydroxide content and fineness on the carbonation of calcium hydroxide*, Constr. Build. Mater., 55, 82-88.

22. Sierra-Fernández, A., Gomez-Villalba, L.S., Milosevic, O., Fort, R., Rabanal, M.E., (2014). *Synthesis ans Morpho-structural charcterization of nanostructures magnesium hydroxide obtained by hydrothermal method*, Ceram. Int. (in press).

23. Wang, Q., Li, C., Guo, M., Sun, L., Hu, C., (2014). *Hydrothermal synthesis of hexagonal magnesium hydroxide nanoflakes*, Mater. Res. Bull., 51, 35-39.

24. Zhang, Y.,Ma, M., Zhang, X., Zhang, B., Wang, B., Liu, R., (2014), *Synthesis, characterization, and catalytic property of nanosized MgO flakes with different shapes*, J. Alloy. Compd., 590, 373-379.